Optics Communications 414 (2018) 98–101

Contents lists available at ScienceDirect

Optics Communications

journal homepage: www.elsevier.com/locate/optcom

High efficiency all-optical plasmonic diode based on a nonlinear side-coupled waveguide–cavity structure with broken symmetry

Hong-Qin Liang, Bin Liu *, Jin-Feng Hu, Xing-Dao He

Jiangxi Engineering Laboratory for Optoelectronics Testing Technology, Nanchang HangKong University, China

ARTICLE INFO

Keywords:
Surface plasmon
All-optical diode
Nonreciprocal transmission
Finite-difference time-domain method

ABSTRACT

An all-optical plasmonic diode, comprising a metal–insulator–metal waveguide coupled with a stub cavity, is proposed based on a nonlinear Fano structure. The key technique used is to break structural spatial symmetry by a simple reflector layer in the waveguide. The spatial asymmetry of the structure gives rise to the nonreciprocity of coupling efficiencies between the Fano cavity and waveguides on both sides of the reflector layer, leading to a nonreciprocal nonlinear response. Transmission properties and dynamic responses are numerically simulated and investigated by the nonlinear finite-difference time-domain method. In the proposed structure, high-efficiency nonreciprocal transmission can be achieved with a low power threshold and an ultrafast response time (subpicosecond level). A high maximum transmittance of 89.3% and an ultra-high transmission contrast ratio of 99.6% can also be obtained. The device can be flexibly adjusted for working wavebands by altering the stub cavity length.

1. Introduction

All-optical diodes are nonreciprocal transmission structures that break time-reversal symmetry; these diodes are highly desirable as building blocks for next-generation all-optical signal processing circuits, which provide analogues to electrical diodes that have enabled modern computer and information technology [1]. However, these schemes still feature some deficiencies. In 1994, Michael Scalora was the first to present an all-optical diode that uses one-dimensional nonlinear photonic crystals [2,3]. Recently, various all-optical diode designs have been proposed including two-dimensional nonlinear photonic crystal micro-cavities with asymmetric structures [4–6], left-handed periodic structures [7], light-tunneling heterostructures with one-dimensional photonic crystals and lossy metallic film [8], asymmetric nonlinear absorption material layers [9], and photonic crystal fibers [10].

Surface plasmon polaritons (SPPs) are electromagnetic surface waves that travel along the interface between metal and dielectrics with exponential decays at both sides. Given that SPPs can overcome the limit of traditional optical diffraction and manipulate optical waves on sub-wavelength scales, SPPs are considered to feature various applications in the development of integrated photonic devices [11]. Various plasmonic devices have been experimentally or theoretically studied [12–17], and all-optical diodes based on plasmonic structures have been proposed and also studied recently [18–21]. However, the overall performance of these all-optical plasmonic diodes still shows deficiencies to a certain degree. Hence, the design of high-efficiency, all-optical plasmonic diodes poses an important challenge.

In this study, we propose and investigate an ultra-compact nonlinear cavity waveguide plasmonic structure, exploiting ultrafast carrier nonlinearities in combination with spatial symmetry breaking to realize nonreciprocal transmission characteristics, as an all-optical diode. The transmission characteristics are simulated by the nonlinear finite-difference time-domain (FDTD) technique, and important all-optical diode performance parameters, including maximum transmittance, transmission contrast ratio between forward and backward transmissions, power threshold, and response time, are systematically analyzed.

2. The model

Fig. 1(a) shows that the all-optical plasmonic diode structure consists of a metal–insulator–metal (MIM) waveguide side-coupled to a plasmonic stub cavity with nonlinear optical Kerr material. A reflecting layer g is set in the MIM waveguide, which slightly deviates from the center position of the stub cavity. d refers to the width of the MIM waveguide, and w represents the distance between the MIM waveguide and stub cavity. g and e indicate the thickness of the reflecting layer and the transverse distance between the center of the reflecting layer and stub cavity, respectively. L_1 and L_2 depict the length and width of

* Corresponding author.
E-mail address: liubin@nchu.edu.cn (B. Liu).

https://doi.org/10.1016/j.optcom.2017.12.081
Received 5 October 2017; Received in revised form 30 November 2017; Accepted 29 December 2017
0030-4018/

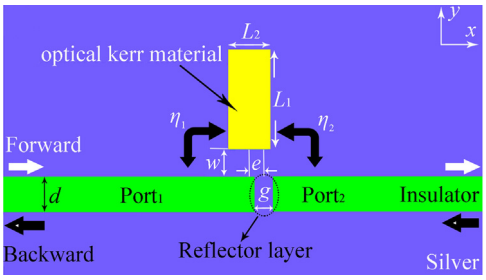

Fig. 1. Schematic diagram of all-optical plasmonic diode based on the MIM waveguide.

stub cavity, respectively. A refractive index of 1.52 (e.g., fused silica) is denoted by the green area, and the blue area accounts for silver. The dispersion equation of SPPs in the MIM structure can be described as follows [22]:

$$\frac{\varepsilon_0 P}{\varepsilon_m k} = \frac{1-\exp(kd)}{1+\exp(kd)}, \quad k = (\beta^2 - \varepsilon_0 k_0^2)^{1/2}, \quad p = (\beta^2 - \varepsilon_m k_0^2)^{1/2}, \tag{1}$$

where β indicates the propagation constant of SPPs, $k_0 = \frac{2\pi}{\lambda}$ is the wave number of light in air, and λ corresponds to the wavelength of incident light. ε_0 and ε_m account for the dielectric constants of the insulator and silver, respectively. The frequency-dependent complex relative permittivity of silver is characterized by the Drude model [23]:

$$\varepsilon_m = \varepsilon_\infty - \frac{\omega_p^2}{\omega^2 + i\gamma\omega}, \tag{2}$$

where $\varepsilon_\infty = 3.7$ stands for the dielectric constant at an infinite angular frequency, $\omega_p = 9.1$ eV is the bulk plasma frequency, which represents the natural frequency of oscillations of free conduction electrons, and $\gamma = 0.018$ eV corresponds to the damping frequency of oscillations. ω pertains to the angular frequency of incident light. The gap of the stub cavity is filled with nonlinear organic polymers, whose dielectric constant ε_c depends on the intensity of the electric field $|E^2|$: $\varepsilon_c = \varepsilon_0 + \chi^{(3)}|E^2|$. The value of the linear dielectric constant ε_0 is set as 2.31, and a typical third-order nonlinear susceptibility is $\chi^{(3)} = 1.4\times10^{-7}$ esu $\approx 1\times10^{-15}$ m^2/V^2 [17]. Our plasmonic device also can be fabricated just like a typical plasmonic microstructures [24]. First, hundreds of nm-thick gold/silver film was prepared using a laser molecular beam epitaxy growth system. Then the desired microstructure was patterned through a focused ion beam etching system. In addition, an input-coupling grating at the input port of each plasmonic slot waveguide and decoupling grating at the terminal region of the output waveguide with an about 100-nm-deep triangular air groove also should be fabricated for conveniently exciting SPP and coupling the SPP mode into free space.

3. Numerical simulation results and discussion

First, we consider a simple side-coupled stub resonator based on the MIM waveguide [Fig. 2(a)]. Transmission characteristics without nonlinear effects are simulated by the FDTD method under linear conditions. The grid size in the x and y directions measures as 2 nm × 2 nm, which is precise enough for the following FDTD simulation. The transmission spectrum in Fig. 2(b) shows the reflecting peak of the stub resonator, whose magnetic field distribution is highly localized in the stub cavity at 945 nm. When the cavity medium is a third-order nonlinear Kerr material, the nonlinear effect can be effectively enhanced. Then, we add a reflector layer to the MIM waveguide below the stub cavity to block waveguides [Fig. 2(c)]. The thickness of the reflector layer is set at g = 20 nm. Fig. 2(d) displays the transmission spectrum without nonlinear effects. A transmission-type Fano resonant peak is obtained at 937 nm as opposed to the original reflecting peak. The Fano resonant wavelength can be effectively adjusted by changing the length of the stub cavity. Hence, our device can be flexibly adjusted for the working waveband by altering the stub cavity length. The Fano resonance may take place under the interference between the continuum traveling mode and the discrete cavity mode [21]. The great difference of the mode amplitudes between the traveling mode and the cavity mode resulting in very weak interference between these two different modes. But, pronounced Fano resonance can occurs when these two types of modes have almost the same amplitudes. The asymmetrical Fano line shape has an asymmetric profile with a dip, resulting from the destructive interference, and a peak, resulting from the constructive interference. In this case, there is a relatively sharp jump of transmittance from dip to peak. Recent reviews have reported comprehensive and detailed descriptions of the Fano resonance in plasmonic nanostructures [25].

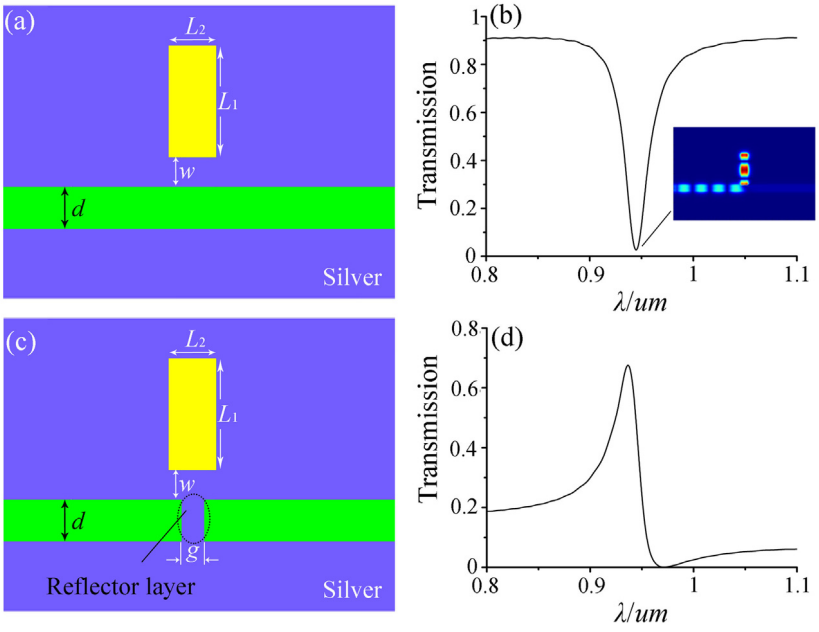

Fig. 2. (a) Schematic diagram and (b) transmission spectrum of a side-coupled stub resonator based on the MIM waveguide; (c) schematic diagram and (d) transmission spectrum after adding a reflector layer.